The American Journal of Human Genetics, Volume *104*

Supplemental Data

Conformational Dynamics and Allosteric Regulation Landscapes of Germline *PTEN* Mutations Associated with Autism Compared to Those Associated with Cancer

Iris Nira Smith, Stetson Thacker, Marilyn Seyfi, Feixiong Cheng, and Charis Eng

Supplemental Data

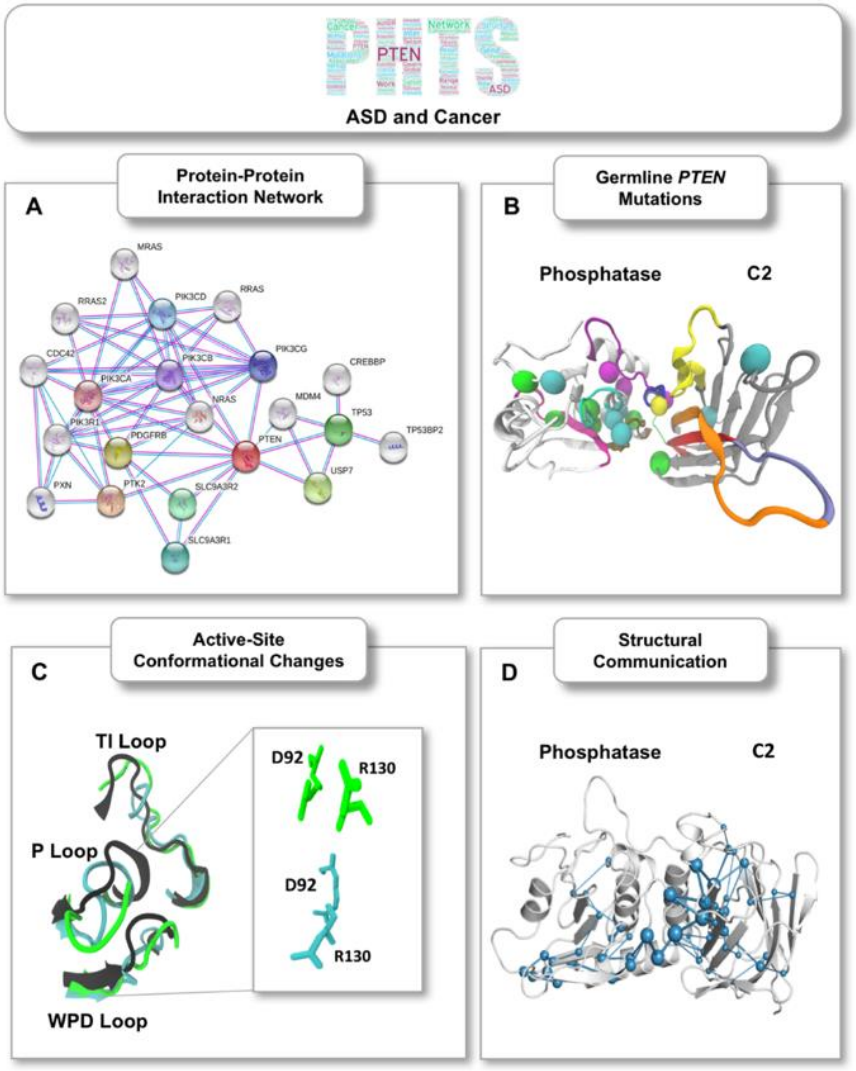

Figure S1. Schematic illustration of network-centric and molecular simulations computational approach supporting interrogation of structural communication and network perturbations in ASD and cancer. (A) PTEN Protein-protein interaction network perturbation analysis. (B) Three-dimensional structural representation of germline *PTEN* mutations associated with ASD and cancer. (C) Conformational analysis of active-site region. (D) Long-range structural communication analysis.

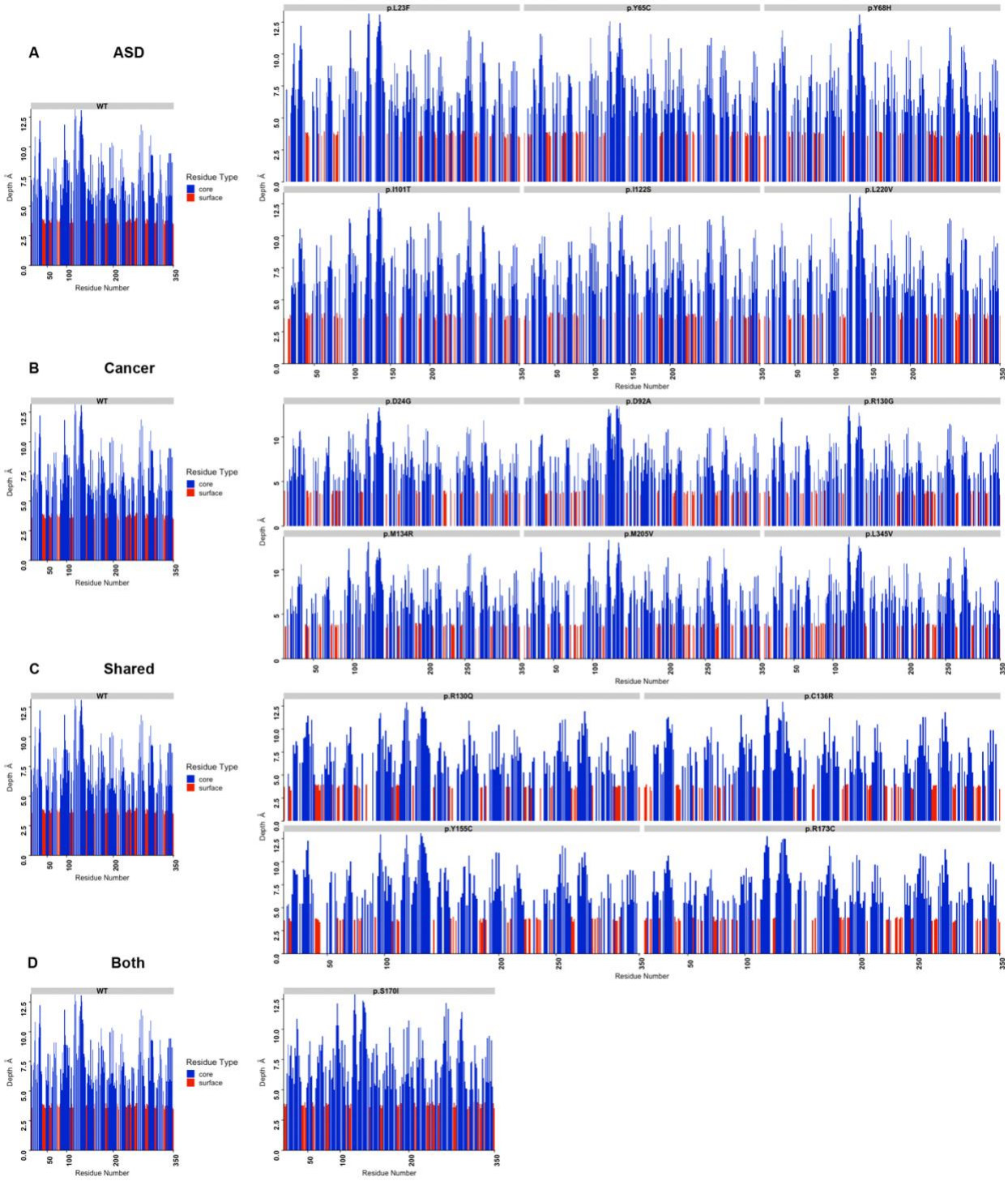

Figure S2. Residue depth profiles across entire PTEN structure for ASD- and Cancer-associated germline *PTEN* mutations. (A) ASD only, (B) cancer only, (C)

mutations shared across both phenotypes, and (D) one mutation with co-existing ASD and cancer. Core and surface residues are indicated in blue and red, respectively.

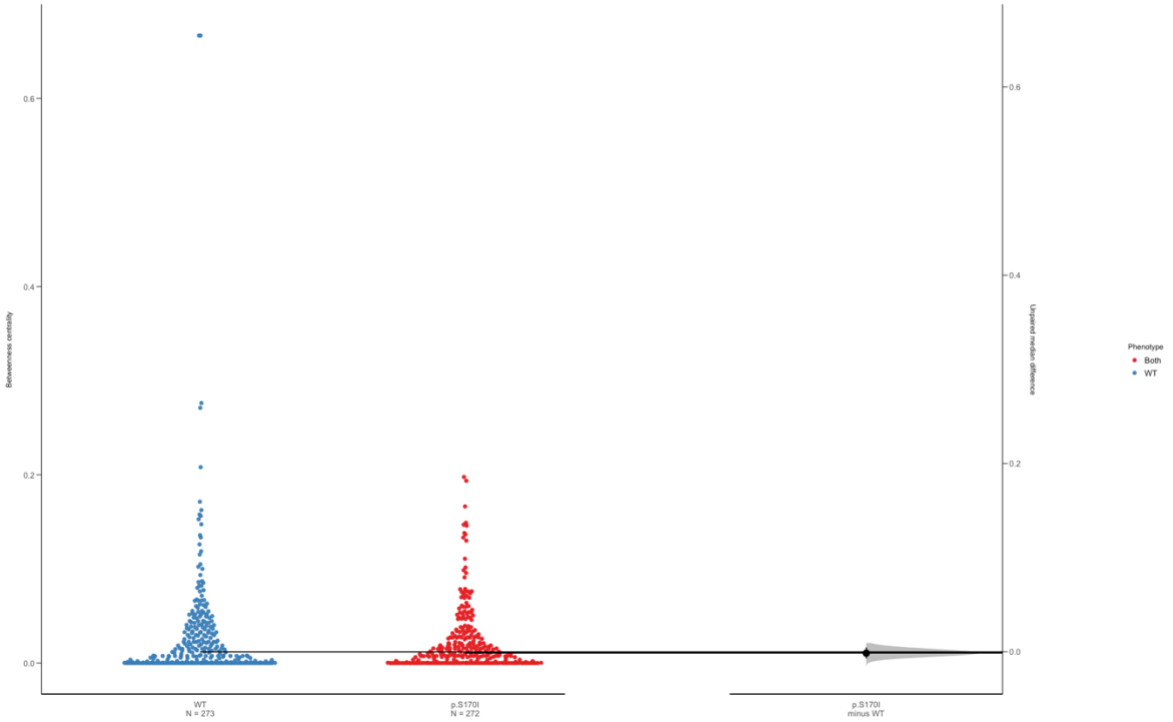

Figure S3. Residue-based betweenness centrality estimation plot profile for co-existing ASD and cancer associated *PTEN* germline mutations. Dynamics-based analysis of betweenness network centrality for one mutation with co-existing ASD and cancer (both). The grey filled curve indicates the complete Δ distribution, given the observed data. In-line with the median of each group, the Δ is indicated by the black circle. The 95% confidence interval of Δ is illustrated by the vertical black line.

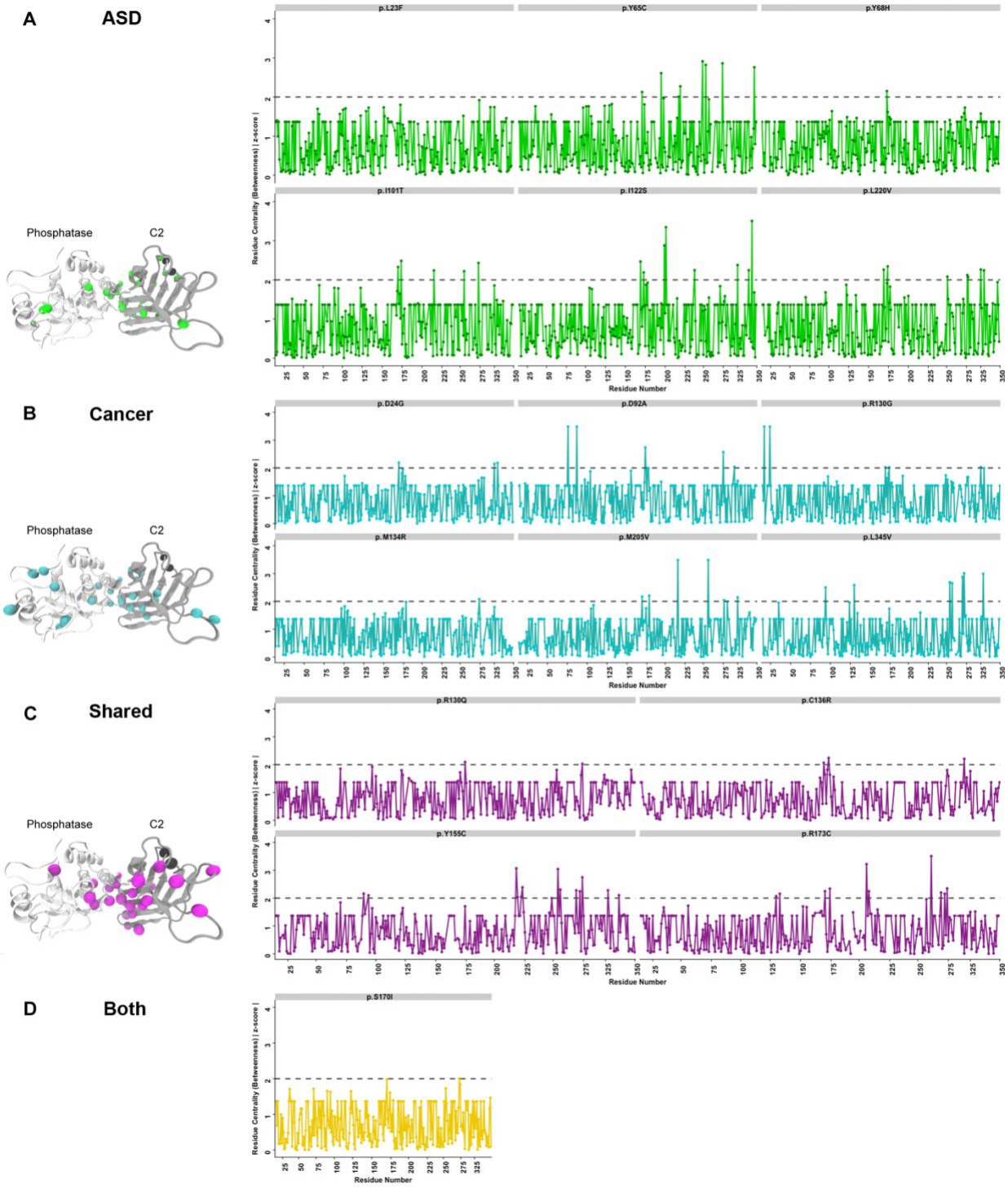

Figure S4. Residue-based betweenness centrality profiles for ASD- and cancer-associated *PTEN* germline mutations. Dynamics-based analysis of betweenness network centrality for (A) ASD only (green), (B) cancer only (cyan), (C) mutations

shared across both phenotypes (magenta), and (D) one mutation with co-existing ASD and cancer (yellow). Critical nodes were evaluated by computing betweenness z-score values versus the corresponding residues with a cutoff threshold of absolute value of 2. Significant betweenness centrality peaks were mapped to the three-dimensional PTEN structure for each phenotype (insets).

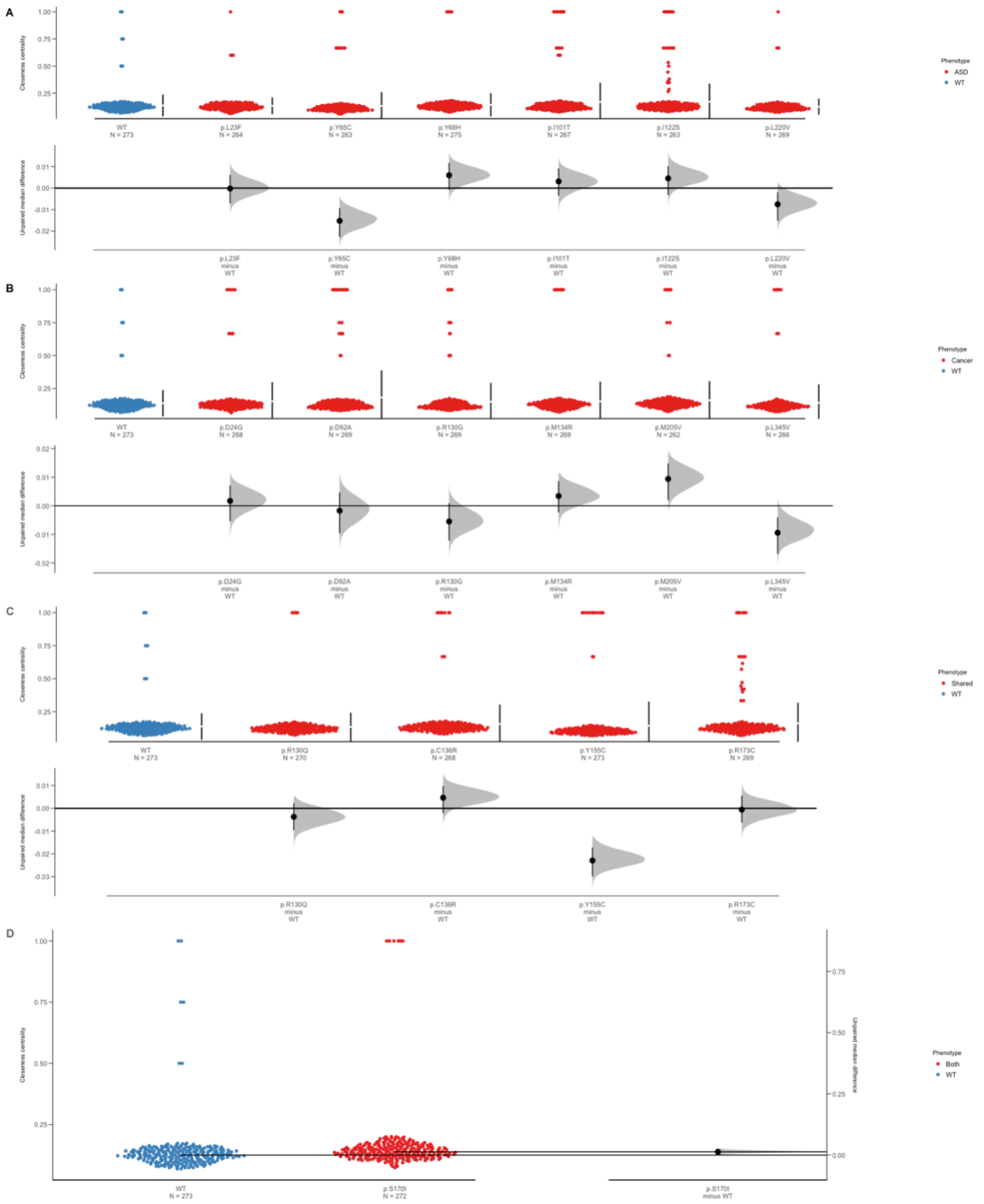

Figure S5. Residue-based closeness centrality estimation plot profiles for ASD- and cancer-associated *PTEN* germline mutations. Dynamics-based analysis of betweenness network centrality for (A) ASD only, (B) cancer only, (C) mutations shared

across both phenotypes, and (D) one mutation with co-existing ASD and cancer. The grey filled curve indicates the complete Δ distribution, given the observed data. In-line with the median of each group, the Δ is indicated by the black circle. The 95% confidence interval of Δ is illustrated by the vertical black line.

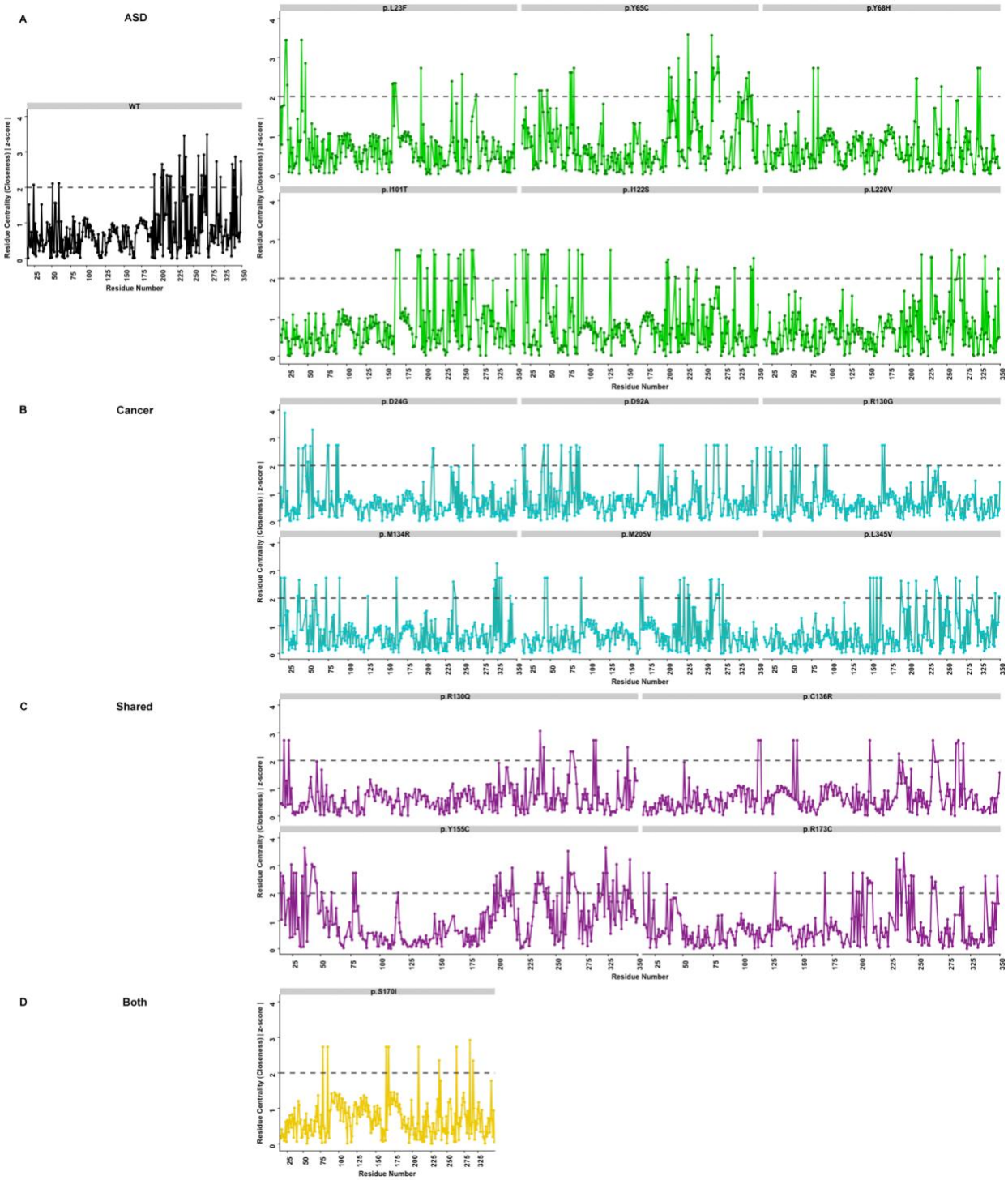

Figure S6. **Residue-based closeness centrality profiles for ASD- and cancer-associated *PTEN* germline mutations.** Dynamics-based analysis of closeness network centrality for (A) ASD only (green), (B) cancer only (cyan), (C) mutations

shared across both phenotypes (magenta), and (D) one mutation with co-existing ASD and cancer (yellow). Critical nodes were evaluated by computing closeness absolute z-score values versus the corresponding residues with a cutoff threshold of absolute value of 2.

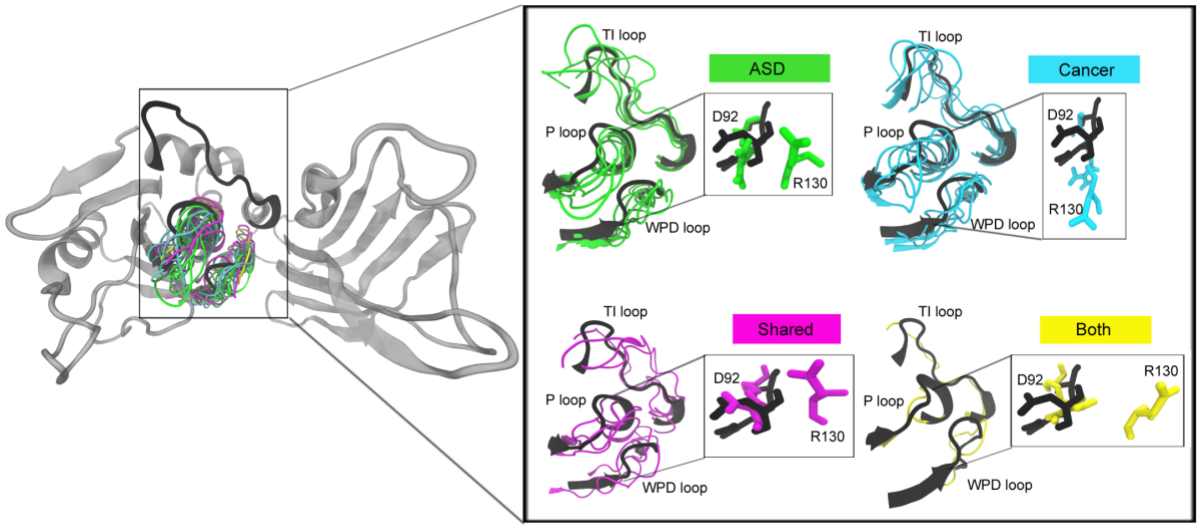

Figure S7. Distinct conformational changes of catalytic active site loops in ASD- and cancer-associated mutations. Conformational changes are indicated in a collapsed representation of the catalytic P-, WPD-, and TI-loops in ASD only (green), cancer only (cyan), mutations shared across both phenotypes (magenta), and one mutation with coexisting phenotypes (yellow) in comparison to WT PTEN (black). Catalytic residues D92 and R130 are indicated in the separate exploded box depicting the orientations as a result of the mutation and subsequent conformational change.

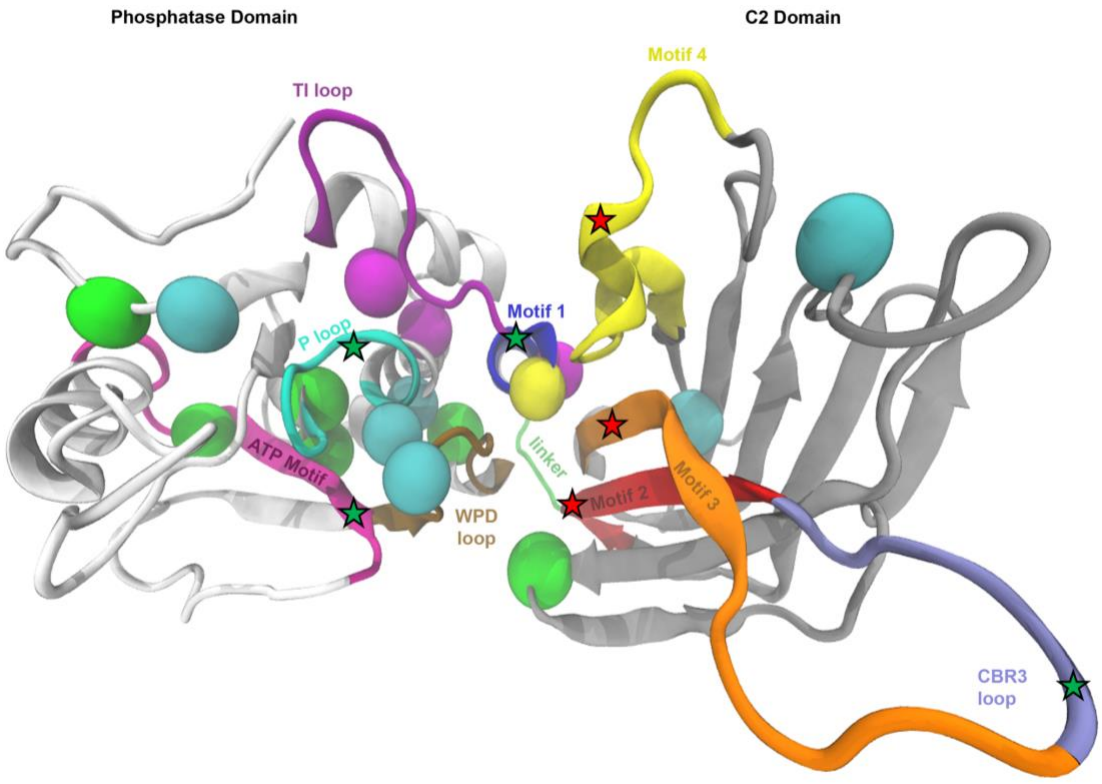

Figure S8. Mapping of critical regions of connectivity in ASD- and cancer-associated mutations on PTEN three-dimensional structure. Individual spheres correspond to 17 germline missense *PTEN* mutations represented by ASD only (green), cancer only (cyan), mutations shared across both phenotypes (magenta), and one mutation with co-existing ASD and cancer (yellow). Critical loops and motifs are labelled as follows: ATP-B binding motif (residues 60-73, pink); WPD loop (residues 88-98, brown); P loop (residues 123-131, cyan); TI loop (residues 160-171, purple); Motif 1 (residues 169-180, blue); Motif 2 (residues 250-259, red); Motif 3 (residues 264-276, orange) Motif 4 (residues 321-334, yellow); CBR3 loop (residues 260-269, ice blue); and Domain linker (residues 185-191, green). Inversely correlated regions (**Table 1**) are designated with stars indicating a 20% increase (red) or decrease (green) compared to the WT.

Table S1. Network proximity (z-score) of PTEN influencers with cancer.

Cancer types	Network proximity (z-score)	
	Somatic mutated genes	Germline mutated genes
BLCA	-5.37193	-3.52376
BRCA	-5.41424	-6.16259
COAD	-5.42926	-5.17049
GBM	-5.03282	-3.74066
LUAD	-5.33628	-5.66893
LUSC	-3.85092	-5.51502
OV	-4.1207	-5.66751
PRAD	-5.28076	-6.12764
SKCM	-4.82602	-4.71384
STAD	-4.07305	-3.31335
THCA	-5.04533	-4.7349
UCEC	-5.90411	-3.38584

Note: 12 cancer types: urothelial bladder carcinoma (BLCA), invasive breast carcinoma (BRCA), colon adenocarcinoma (COAD), glioblastoma multiforme (GBM), lung adenocarcinoma (LUAD), lung squamous cell carcinoma (LUSC), ovarian serous cystadenocarcinoma (OV), prostate adenocarcinoma (PRAD), skin cutaneous melanoma (SKCM), stomach adenocarcinoma (STAD), papillary thyroid carcinoma (THCA), and uterine corpus endometrial carcinoma (UCEC). Based on our previous study, z-score less than -2.0 represent a significant network proximity (p-value less than 0.05 by permutation test).

Table S2. PSG interaction strength (I_{min}) network parameter

PSG	I_{min}[a]
p.L23F	3.03
p.Y65C	2.86
p.Y68H	3.25
p.I101T	3.93
p.I122S	2.88
p.L220V	3.76
p.D24G	2.34
p.D92A	2.77
p.R130G	3.00
p.M134R	2.94
p.M205V	2.82
p.L345V	3.49
p.R130Q	3.35
p.C136R	3.72
p.Y155C	2.52
p.R173C	2.97
p.S170I	3.57

[a]Interaction strength cutoff (%)